The rotation-tunneling spectrum of 3-hydroxypropenal and confirmation of its detection toward IRAS 16293-2422 B

H. S. P. Müller, A. Coutens, J. K. Jørgensen, L. Margulès, Roman A. Motiyenko, Jean-claude Guillemin

A&A, 687, A8 (2024)
https://doi.org/10.1051/0004-6361/202450029

Astronomy & Astrophysics

The rotation-tunneling spectrum of 3-hydroxypropenal and confirmation of its detection toward IRAS 16293−2422 B⋆

H. S. P. Müller[1], A. Coutens[2], J. K. Jørgensen[3], L. Margulès[4], R. A. Motiyenko[4], and J.-C. Guillemin[5]

[1] Astrophysik/I. Physikalisches Institut, Universität zu Köln, Zülpicher Str. 77, 50937 Köln, Germany
e-mail: hspm@ph1.uni-koeln.de
[2] Institut de Recherche en Astrophysique et Planétologie (IRAP), Université de Toulouse, UT3-PS, CNRS, CNES, 9 av. du Colonel Roche, 31028 Toulouse Cedex 4, France
[3] Niels Bohr Institute, University of Copenhagen, Øster Voldgade 5−7, 1350 Copenhagen K, Denmark
[4] Univ. Lille, PhLAM – Physique des Lasers, Atomes et Molécules, CNRS, UMR 8523, 59000 Lille, France
[5] Univ Rennes, Ecole Nationale Supérieure de Chimie de Rennes, CNRS, ISCR−UMR 6226, 35000 Rennes, France

Received 19 March 2024 / Accepted 30 April 2024

ABSTRACT

Context. 3-Hydroxypropenal (HOCHCHCHO) is the lower energy tautomer of malonaldehyde which displays a complex rotation-tunneling spectrum. It was detected somewhat tentatively toward the solar-type protostellar system IRAS 16293−2422 with ALMA in the framework of the Protostellar Interferometric Line Survey (PILS). Several transitions, however, had large residuals, preventing not only their detection, but also the excitation temperature of the species from being determined unambiguously.
Aims. We want to extend the existing rotational line list of 3-hydroxypropenal to shed more light on the recent observational results and to facilitate additional radio astronomical searches for this molecule.
Methods. We recorded and analyzed the rotation-tunneling spectrum of 3-hydroxypropenal in the frequency regions between 150 and 330 GHz and between 400 and 660 GHz. Transitions were searched for in the PILS observations of IRAS 16293−2422. Local thermodynamic equilibrium (LTE) models were carried out and compared to the observations to constrain the excitation temperature. Additional transitions were searched for in other ALMA archival data of the same source to confirm the presence of 3-hydroxypropenal.
Results. More than 7500 different spectral lines, corresponding to more than 11 500 transitions, were assigned in the course of our investigation with quantum numbers $2 \le J \le 100$, $K_a \le 59$, and $K_c \le 97$, resulting in a greatly improved set of spectroscopic parameters. The comparison between the LTE models and the observations yields an excitation temperature of 125 K with a column density $N = 1.0 \times 10^{15}$ cm^{-2} for this species. We identified seven additional lines of 3-hydroxypropenal that show a good agreement with the model in the ALMA archive data.
Conclusions. The calculated rotation-tunneling spectrum of 3-hydroxypropenal has sufficient accuracy for radio astronomical searches. With the solution of the excitation temperature conundrum and the detection of seven more lines, we consider the detection of 3-hydroxypropenal toward IRAS 16293−2422 as secure.

Key words. molecular data – methods: laboratory: molecular – techniques: spectroscopic – radio lines: ISM – ISM: molecules – astrochemistry

1. Introduction

Malonaldehyde is the prototype and parent species of β-dicarbonyl compounds of the form RC(O)CH$_2$C(O)R′ (R = R′ = H for malonaldehyde). However, it was found that enol tautomers of these molecules were usually lower in energy because of the formation of intramolecular hydrogen bonds. An interesting question in the special case of R = R′ was if this hydrogen bonding was strong enough to form symmetric hydrogen bonds to both oxygen atoms or if the bonding was weaker to form a hydrogen bond with only one oxygen atom, thus yielding a double minimum potential possibly with tunneling between the two minima. The enol tautomer of malonaldehyde is 3-hydroxypropenal, one of the simplest molecules containing a ring which is closed by a hydrogen bond. Early quantum-chemical calculations yielded contradicting results on its structure; Karlström et al. (1975) found a structure with an asymmetric double minimum potential with a barrier low enough to permit tunneling between the two minima, as presented in the left and right parts of Fig. 1, whereas Isaacson & Morokuma (1975) found a structure with a single, symmetric minimum potential, such as the one shown in the center of Fig. 1.

The rotational spectra of several 3-hydroxypropenal isotopologs were investigated extensively in order to resolve this conflict. Two sets of transitions with similar spectroscopic parameters, but opposing spin-statistics (3:1 versus 1:3) were identified in an early, preliminary account (Rowe et al. 1976). The second set belonged to a state 16 ± 14 cm^{-1} higher than that of the first set, compatible with a double minimum potential with tunneling and almost certainly ruling out a symmetric single minimum potential. Comparison of the OO non-bonding distance, determined through ^{16}O/^{18}O substitution, with values from quantum-chemical calculations (Karlström et al. 1975; Isaacson & Morokuma 1975) supported this interpretation. Baughcum et al. (1981) investigated many more isotopic species, extended the measurements into the lower millimeter region, carried out dipole moment measurements, refined the energy

⋆ Supplementary data are available at CDS via anonymous ftp to cdsarc.cds.unistra.fr (130.79.128.5) or via https://cdsarc.cds.unistra.fr/viz-bin/cat/J/A+A/687/A8

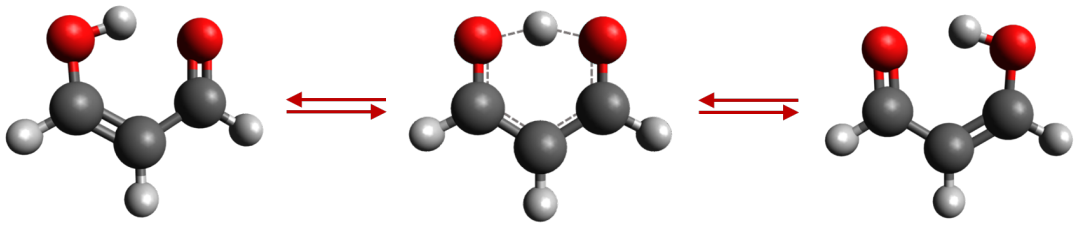

Fig. 1. Model of the 3-hydroxypropenal molecule. Carbon atoms are symbolized by gray spheres, hydrogen atoms are indicated by small, light gray spheres, and oxygen atoms by red spheres. The two equivalent minimum structures are shown at the outside while the transition state with C_{2v} symmetry is displayed in the center.

difference of the two states to 26 ± 10 cm^{-1} and observed an absorption band near 21 cm^{-1} for the main isotopolog, and determined the structural parameters of the asymmetric minimum configuration of 3-hydroxypropenal. Two later studies (Baughcum et al. 1984; Turner et al. 1984) improved the analyses of the rotation-tunneling interaction and reported additional transition frequencies for the main isotopolog (Turner et al. 1984). Baughcum et al. (1984) also evaluated the tunneling barrier height for the main isotopolog as ∼6.6 kcal mol^{-1} or ∼2300 cm^{-1}.

Stolze et al. (1983) studied the rotational Zeeman effect of 3-hydroxypropenal and reported field-free transition frequencies for some low-J transitions. Firth et al. (1991) applied tunable far-infrared spectroscopy to extend transition frequencies of the main isotopolog into the submillimeter region. Finally, Baba et al. (1999) reported several transition frequencies between the two tunneling states and evaluated the associated a-dipole moment component through relative intensity measurements in comparison to the rotational transitions within the tunneling states, which obey b-type selection rules.

Recently, Coutens et al. (2022) employed a catalog entry of the Cologne Database for Molecular Spectroscopy, (CDMS, Müller et al. 2005; Endres et al. 2016) to identify 3-hydroxypropenal somewhat tentatively toward the B component of the protostellar system IRAS 16293−2422 (hereafter IRAS16293) in observations with the Atacama Large Millimeter/submillimeter Array (ALMA) obtained in the Protostellar Interferometric Line Survey (PILS), an unbiased molecular line survey between 329.1 and 362.9 GHz (Jørgensen et al. 2016). The 3-hydroxypropenal catalog entry had one decisive drawback that transition frequencies in the frequency range of the survey with low values of K_a had rather large uncertainties, preventing to establish their presence or absence. Such transitions should be observable in the warm excitation temperature scenario of ∼300 K, whereas they should be too weak to be identified in the luke-warm excitation scenario of ∼125 K. Both excitation scenarios were found quite commonly for molecules identified in PILS (e.g., Jørgensen et al. 2018).

We have recorded and analyzed the rotation-tunneling spectrum of 3-hydroxypropenal in the millimeter and submillimeter region in order to establish its excitation temperature in IRAS16293 B, which may lead to greater certainty about the presence of the molecule in this source, and to facilitate further searches for 3-hydroxypropenal in the interstellar medium.

We provide in Sect. 2 the spectroscopic properties of the molecule, in Sect. 3 the experimental details, describe in Sect. 4 the laboratory spectroscopic results, and discuss these in Sect. 5. The astronomical observations are detailed in Sect. 6, and conclusions and outlook are presented in Sect. 7.

2. Spectroscopic properties of 3-hydroxypropenal

The 3-hydroxypropenal molecule is a very asymmetric rotor of the prolate type with $\kappa = (2B - A - C)/(A - C) = -0.4441$. It has two equivalent configurations of C_S symmetry, as displayed schematically in Fig. 1. The barrier to interchange between these two minima is sufficiently low to facilitate tunneling, which leads to a symmetric tunneling state $v = 0^+$ and an antisymmetric tunneling state $v = 0^-$ 647046.2 MHz higher in energy (Baba et al. 1999). The transition state of C_{2v} symmetry is shown in the center of Fig. 1. The two equivalent H atoms not on the symmetry axis in the transition state lead to ortho/para spin-statistics with relative intensities of 3:1. The ortho levels in $v = 0^+$ are those with $K_a + K_c$ being odd and in $v = 0^-$ those with $K_a + K_c$ being even.

The dipole moment component for rotational transitions, within $v = 0^+$ or $v = 0^-$, is along the b-axis, the symmetry axis of the transition state. Its magnitudes were determined through Stark spectroscopy as μ_b = (2.59 ± 0.02) D for $v = 0^+$ and μ_b = (2.58 ± 0.02) D for $v = 0^-$ (Baughcum et al. 1981). The selection rules are $\Delta J = 0, \pm 1$ and ΔK_a and ΔK_c are odd. The strongest transitions are ^rR-branch transitions with $\Delta K_a = +1$ and $\Delta J = +1$ from the lower to the upper state and K_a close to J. Such transitions were reported by Firth et al. (1991) in their tunable far-infrared study; transitions with very low values of K_a were not reported. Also at lower K_a, ^pR-branch transitions ($\Delta K_a = -1$) are relatively strong as they form asymmetry doublets with the ^rR-branch transitions having the same J and K_c. The respective pair of transitions is well separated at intermediate K_a and K_c, but the splitting decreases rapidly with decreasing K_a and is collapsed well before $K_a = 0$. This pairing of asymmetry doublets is called oblate pairing while the respective pairing at high values of K_a is called prolate pairing. The Q-branch transitions ($\Delta J = 0$) are usually weaker, but higher-J may appear as quite strong compared to lower-J R-branch transitions, which is quite commonly found at lower frequencies. The P-branch transitions ($\Delta J = -1$) are usually weaker still. Finally, the asymmetry of the molecule causes transitions with $\Delta K_a = \pm 3$ etc. to have non-negligible intensities.

The tunneling of the H atom is along the a-axis; transitions between $v = 0^+$ and $v = 0^-$ follow therefore a-type selection rules with $\Delta J = 0, \pm 1$, ΔK_a even, and ΔK_c odd. Strong rotation-tunneling transitions are ^qQ-branch transitions with K_a close to J. The transitions reported by Baba et al. (1999) were mostly of this type as they occur in a rather narrow frequency window quite close to the tunneling frequency. A small number of transitions with somewhat lower values of K_a were not included in their fit because they were weak or blended. And again were transitions with very low values of K_a not reported in that work.

Baba et al. (1999) determined $\mu_a/\mu_b = 0.14$ from relative intensity measurements. This yields $\mu_a = 0.36$ D; it was assumed that μ_a is positive, as is commonly done. The intensities of transitions involving at least one perturbed level may, however, be affected by the sign of μ_a relative to that of μ_b and that of F_{ab}, as will be discussed in Sect. 4.3. Also relatively strong are ${}^qP$- and ${}^qR$-branch transitions having low values of K_a. The ${}^qR$-branch transitions have frequencies above the tunneling frequency for the most part while ${}^qP$-branch transitions are usually found below it. Transitions with $\Delta K_a = \pm 2$ etc. gain considerable intensity because of the asymmetry of the 3-hydroxypropenal molecule. In addition, they may borrow additional intensity from rotational transition through tunneling-rotation interaction.

Energy levels in $v = 0^+$ and $v = 0^-$ with similar energies can interact if they have the same J and if they differ in K_a by an odd number and in K_c by an even number. The interaction is a Coriolis-type interaction, frequently just called Coriolis interaction. It is usually strongest the closer the energies are in the unperturbed case, the smaller ΔK_a and ΔK_c are, and the higher J and K_a or K_c are. Consequences of the interactions are that the two levels repel each other and mix in character with strength of the interaction. Transitions may be displaced by several gigahertz, and tunneling-rotation transitions can gain also intensity from rotational transitions through the mixing.

3. Experimental details

3.1. Sample preparation

The malonaldehyde synthesis of Trivella et al. (2008) was applied with slight modifications. Acid hydrolysis of 1,1,3,3-tetraethoxypropane (purity > 96%, Sigma Aldrich) followed by treatment with aqueous NaOH gave the sodium salt of malonaldehyde. This salt suspended in diethyl ether was then acidified with an anhydrous solution of HCl in diethyl ether at −40 °C followed by 2 h of stirring at this temperature. Purification was carried out by trap-to-trap distillation with slow heating to room temperature of the solution to give pure malonaldehyde in a trap immersed in a bath cooled to −50 °C.

3.2. Spectroscopic measurements

The measurements between 150 and 330 GHz and between 400 and 660 GHz were carried out with the Lille spectrometer (Zakharenko et al. 2015). We employed a quartz tube (10 cm diameter, 200 cm in length) as absorption cell. Throughout the measurement, the sample was submerged in an ethanol cold bath at −15 °C, and a minimum flow of the sample vapor was maintained between 2.0 to 2.5 Pa (20–25 µbar). The frequencies were covered with various active and passive frequency multipliers from VDI Inc., and an Agilent synthesizer (12.5–18.25 GHz) was used as the source of radiation. A liquid He-cooled InSb bolometer (QMC Instruments Ltd) was used to detect the absorption signals. The uncertainties of the measured line position were judged on the symmetry of the line-shape and the signal-to-noise ratio (S/N); 15, 20, or 30 kHz were assigned to average lines, 10 and 5 kHz for very symmetric lines with very good S/N, and 50, 70, or 100 kHz for weaker lines, lines with poorer S/N, or lines with less symmetric line-shape, for example, because of the proximity to another line.

4. Laboratory spectroscopic results

4.1. Analysis and fitting

The rotation-tunneling spectrum, such as in the case of 3-hydroxypropenal, is usually treated with a Hamiltonian that is divided into a 2×2 matrix. The diagonal elements are commonly two Watson-type rotational Hamiltonians and include the energy of the upper tunneling state; the interaction Hamiltonian is off-diagonal. We applied here Watson's S reduced Hamiltonian in the prolate I^r representation on the diagonal; see Margulès et al. (2020) for a discussion on the advantages of the S reduction.

The two tunneling states 0^+ and 0^- together comprise the ground vibrational state $v = 0$. Therefore, it can be advantageous to rearrange the Hamiltonians and fit average spectroscopic parameters $X = (X(0^+) + X(0^-))/2$ and differences $\Delta X = (X(0^-) - X(0^+))/2$, as was done by Christen & Müller (2003) in their treatment of the lowest energy conformer of ethylene glycol. Christen & Müller (2003) also pointed out that the differences in spectroscopic parameters can be interpreted as rotational corrections to the energy difference. We follow this interpretation in the present work. We should point out that in our definition of the differences, 0^- is higher in energy by $2E$ than 0^+. The advantage of this formulation is that an average parameter or its difference can be used individually in the fit independent of each other and was particularly noteworthy in a refit of ethanethiol data (Müller et al. 2016). Other investigations applying this approach include hydroxyacetonitrile (Margulès et al. 2017) and some of its minor isotopic species (Margulès et al. 2023) as well as dimethylamine (Müller et al. 2023).

The off-diagonal interaction was described employing Pickett's Reduced Axis System (RAS) (Pickett 1972), as was already done in earlier studies of the rotation-tunneling spectrum of 3-hydroxypropenal. The only non-zero low-order term is $F_{ab}(J_aJ_b + J_bJ_a)$ that may be supplemented with suitable distortion parameters of the form $(F_{ab,K}J_a^2 + F_{ab,J}J^2 + F_{2ab}(J_b^2 - J_c^2) + ...) \times (J_aJ_b + J_bJ_a)$.

Pickett's programs SPCAT and SPFIT (Pickett 1991) were used to calculate and fit the rotational spectra of 3-hydroxypropenal. We determined the spectroscopic parameters of 3-hydroxypropenal in the usual way. We tested after each round of assignments if one or more spectroscopic parameters would improve the quality of the fit by amounts that warranted keeping the respective parameter in the fit. This procedure helps to keep the number of spectroscopic parameters small while reproducing the transition frequencies already in the fit as well as possible. It is important to try only parameters that are reasonable with respect to those already used in the fit. If at least one parameter improved the quality of the fit sufficiently, we chose the one that improved the quality the most and searched for additional parameters. We tested occasionally if a parameter with relatively large uncertainties can be omitted from the fit without increasing the rms error of the fit by too large amounts.

4.2. Previous data

We describe the previous data, their treatment in the initial fit that was the basis of the version 1 CDMS catalog entry of 3-hydroxypropenal, which in turn was the starting point of our present analysis, and their treatment in the final fit of the present study. The microwave data from Baughcum et al. (1981) up to

40 GHz displayed very small residuals and were assigned uncertainties of 10 kHz in the initial fit as well as in the final fit of this study since no uncertainties were given in that work. The *b*-type ^{r}R- and ^{r}Q-branch transitions cover quantum numbers $1 \le J \le 15$ and $K_a \le 6$. The millimeter wave transitions between 55 and 113 GHz were ^{r}Q-branch transitions with $6 \le J \le 29$ and $2 \le K_a \le 11$ that were taken with a different spectrometer. Uncertainties of 150 kHz were applied in the initial fit and one transition with $J = 37$ was omitted because of large residuals. These data were omitted in the final fit of the present work because of transition frequencies with similar quantum numbers with much smaller uncertainties.

Stolze et al. (1983) published microwave transitions between 12 and 25 GHz with $K_a \le J \le 3$. They reported uncertainties as being better than 20 kHz. We included them in the initial fit as well as in the final fit from our current investigation with 10 kHz uncertainties.

Turner et al. (1984) reported a moderate number of ^{r}R- and ^{r}Q-branch transitions between 78 and 85 GHz having $8 \le J \le 38$ and $K_a \le 14$ with estimated uncertainties of 200 kHz. The transition frequencies were used in the initial fit except for three. Their data were omitted from our present final fit for the same reason as above.

The tunable far-infrared data published by Firth et al. (1991) are ^{r}R-branch transitions, except for two ^{p}R-branch transitions, distributed between 352 and 898 GHz with $20 \le J \le 50$ and $10 \le K_a \le 44$. Uncertainties were reported to be about 400 kHz, which appeared to be too optimistic. We assigned 800 kHz in our initial fit and omitted three transition frequencies because of large residuals nevertheless. We omitted these data in our final fit because of the large uncertainties and because we have remeasured many of these transition more accurately.

The only tunneling-rotation transitions were reported by Baba et al. (1999). They published ^{q}Q-branch transitions between 643 and 651 GHz with $8 \le J \le 35$ and $4 \le K_a \le 30$. No uncertainties were given explicitly, but the rms of ~30 kHz for their lines included in the fit was deemed to be commensurate with the uncertainties. We included the data in our initial fit accordingly, but omitted them in our final fit of this study. Not only did we redetermine frequencies of most transitions, often with better uncertainties, but we also noted that the series of transitions with $K_a = J - 4$ and $K_a = J - 5$ differed in many cases from our measurements and from the calculated frequencies by 50 kHz and more; only the short series of transitions with $K_a = J$ showed very good agreement with the exception of one line that was not included in their fit and was not assigned in the present work.

4.3. Observed spectrum and assignments

The recorded rotation-tunneling spectrum of 3-hydroxypropenal displayed fluctuations in the S/N, which is commonly observed in millimeter and submillimeter spectroscopy, but the change in S/N is mostly gradual. In combination with a rather rich spectrum, the relative intensity is not only helpful for assignments, but it is also an important tool to judge if a line may be blended. Obviously blended lines were in most cases not included in the line list except for unresolved asymmetry doublets and occasionally accidental blends of lines assignable to the ground vibrational state of 3-hydroxypropenal as long as the line shape was sufficiently symmetric.

Initial assignments were made above 600 GHz because this is the region in which the *a*-type rotation-tunneling transitions occur which were reported by Baba et al. (1999). However, the transitions easily assignable in the first round were *b*-type *R*-branch transitions with $31 \le J \le 50$ and mostly fairly high values of K_a, up to 32. The lowest K_a values by far in this round were those of a $K_a = 12$–9 transition.

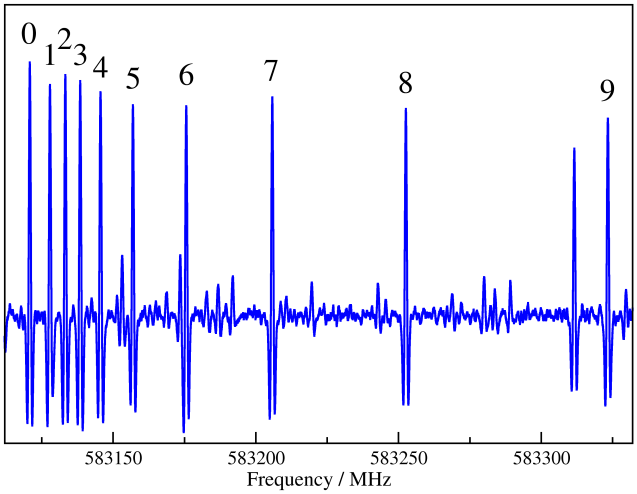

Fig. 2. Section of the rotational spectrum of 3-hydroxypropenal. The transitions are within $v = 0^-$ and have $J_{K_c} = 86$–$n_{86-2n} \leftarrow 85$–n_{85-2n}; the values of n are indicated. Transitions with $K_a = 1$–0 and 0–1 are paired for $n = 0$, those with $K_a = 2$–1 and 1–2 are paired for $n = 1$, and so on.

Not all of the assigned transitions could be fit satisfactorily in the first few rounds. Transitions with large residuals were weighted out temporarily as we assumed these residuals were a consequence of correlation among the interaction parameters and between these and the remaining parameters. Eventually, most of these lines were fit well, the remaining ones were omitted as for most of these closer inspection suggested the lines to be blended. Transitions with modest residuals around three to four times of the experimental uncertainties were marked for occasional inspection. Almost all of these were fit well in later fits.

Subsequently, assignments were made between 500 and 660 GHz in several rounds, slowly increasing the quantum number range and also assigning weaker lines. The second round included *a*-type rotation-tunneling transitions, and soon thereafter, we assigned transitions with low values of K_a at and near the oblate limit, i.e., with K_c near J and J around 80 and 90. A conspicuous clustering of *R*-branch transitions occurs near the oblate limit, as shown in Fig. 2: transition decreasing in J by one, in K_c by two, and increasing in K_a by one occur very close in frequency, the appearance resembling the origin of a *Q*-branch.

We assigned transitions in sections decreasing in frequency afterwards. The clustering of *R*-branch transitions near the oblate limit was a persistent feature, but frequently disrupted for some transitions, as displayed in Fig. 3. The disruption is caused by a $\Delta K_c = 2$ interaction which is resonant at $J = 45$ and $K_c = 43$ in $v = 0^+$ and $K_c = 45$ in $v = 0^-$. The $v = 0^+$ transition with $J_{K_c} = 46_{44} - 45_{43}$ is shifted by ~2 GHz to 331903.2 MHz, in the 330–400 GHz measurement gap.

A plot of the reduced energy $E - (B+C)J(J+1)/2$ versus J is shown in Fig. 4. The purely J-depended effects are subtracted off to first order from the rotational energy such that the combined effects of asymmetry, centrifugal distortion, and perturbation are visible for individual K_a series of $v = 0^+$ and $v = 0^-$. The $\Delta K_c = 2$ interaction is resonant at $K_c = 43$ for $v = 0^+$ and $K_c = 45$ for $v = 0^-$ for $45 \le J \le 48$. The resonant K_c pair increases gradually

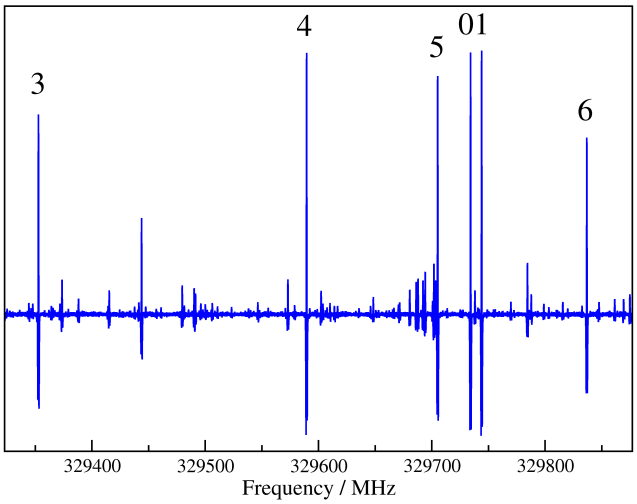

Fig. 3. Section of the rotational spectrum of 3-hydroxypropenal. The transitions are within $v = 0^+$ and have $J_{K_c} = 48$–$n_{48-2n} \leftarrow 47$–n_{47-2n}; the values of n are indicated. The $J_{K_c} = 46_{44} - 45_{43}$ transition ($n = 2$) is shifted by ~2 GHz to higher frequencies.

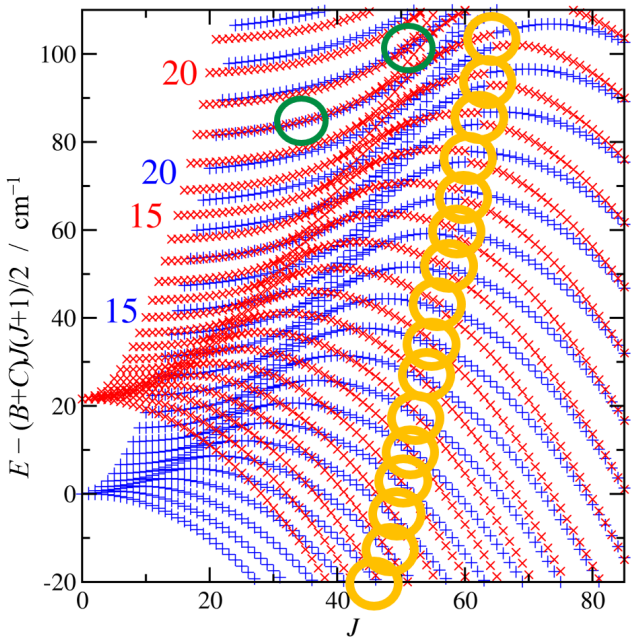

Fig. 4. Section of the reduced energy plot of 3-hydroxypropenal. Data points of $v = 0^+$ are shown in blue, those of $v = 0^-$ in red; selected K_a series are indicated to the left. Resonant interactions with $\Delta K_c = 2$ are indicated by yellow circles. They occur at $K_c = 43$ for $v = 0^+$ and $K_c = 45$ for $v = 0^-$ for $45 \leq J \leq 48$. The resonant K_c pair increases gradually with J, $K_c = 44$ and 46 are resonant for $49 \leq J \leq 58$. Two $\Delta K_a = 3$ interactions are resonant at $K_a = 21/18$ and $J = 35$ as well as $K_a = 22/19$ and $J = 49$ for ortho and $J = 50$ for para, which is signaled by green circles. Further $\Delta K_a = 3$ or 5 interactions are usually more local and are not highlighted.

with J, $K_c = 44$ and 46 are resonant for $49 \leq J \leq 58$, $K_c = 45$ and 47 for $59 \leq J \leq 63$, $K_c = 46$ and 48 for $64 \leq J \leq 66$, and so on. The perturbations are fairly weak and rather local for the lower values of J, the shift in energy is not or only hardly seen in the reduced energy plot. Increasingly larger effects are noticeable in Fig. 4 for $J > 50$. At least two, often many more transitions were included in the line list for each tunneling state and nearly

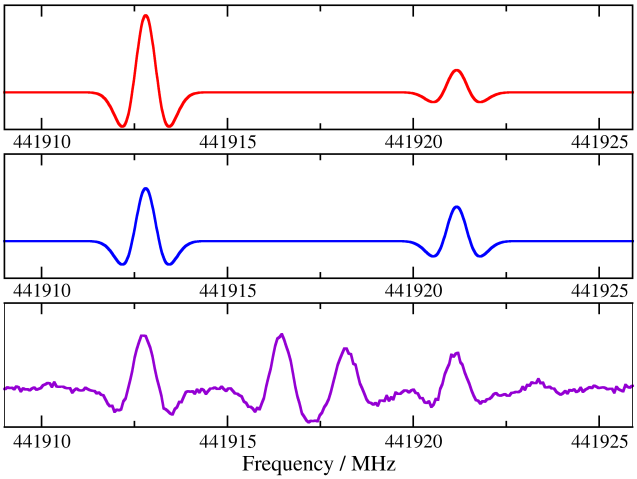

Fig. 5. Section of the rotational spectrum of 3-hydroxypropenal in the lower trace. The $J_{K_a} = 58_{41} - 58_{40}$ transition within $v = 0^-$ is shown to the left, and the $42_{41} - 42_{40}$ transition within $v = 0^+$ to the right. The two transition between them are unassigned. The upper trace shows a simulation of the spectrum with μ_a, μ_b, and F_{ab} chosen to be positive; the sign of μ_a is negative in the middle trace.

all J between 45 and 70, at which point many energy levels with similar quantum numbers are perturbed very strongly, and the attribution of energy levels to $\Delta K_c = 2$ interactions are complex.

We identified other strong interactions which cause perturbations in several values of J, for example, with $\Delta K_a = 3$, which are resonant at $J = 35$ and $K_a = 21$ and 18 for $v = 0^+$ and $v = 0^-$, respectively, and at $J = 49$ and 50 for ortho- and para-3-hydroxypropenal, respectively, in the case of $K_a = 22$ and 19. These resonances are also indicated in Fig. 4. Multiple transitions were assigned for these levels as well as in the vicinity of the resonance for both tunneling states. Other, more local perturbations are best described as connecting levels with $\Delta K_c = 4$, ΔK_a changes by 5 for one asymmetry side and by 3 for the other. Two examples with multiple transitions in the line list are $37_{17,21}$ in $v = 0^+$ and $37_{12,25}$ in $v = 0^-$ or the respective pair $41_{16,26}$ and $41_{11,30}$. The various perturbations may transfer intensity to rotation-tunneling transitions having $\Delta K_a = 2$, 4, and 6.

After having reached the lower frequency limit of 150 GHz in the assignment process, further assignments were made by going up in frequency to the upper limit. The assignments involved often weak lines, but also some stronger lines whose assignments were uncertain initially because they were calculated too far away from their frequency in the experimental spectrum. In addition, few transitions were checked that had relatively large residuals in the fit. Among the weak transitions included in the line list are b-type Q-branch rotational transitions with K_a up to 59. Some of these displayed a fairly strong dependence on the sign choice of μ_a with μ_b and F_{ab} chosen to be positive, as can be seen in Fig. 5. The upper trace simulation shows two lines differing in intensity by a factor of ~3.5 whereas in the middle trace simulation the factor is only ~1.5, which is clearly more appropriate. These intensity changes upon sign change of μ_a were among the largest easily discernible in the spectrum.

Our final line list consisted of 11551 transitions from the present study which correspond to 7551 different frequencies, mostly because of unresolved asymmetry splitting. The quantum numbers J, K_a, and K_c reach values of 100, 59, and 97. The numbers of transitions within $v = 0^+$ and $v = 0^-$ is 5123 and 5127, respectively, most having $\Delta K_a = \pm 1$, some have $\Delta K_a = 3$. There

Table 1. Average spectroscopic parameters X (MHz) and energy E with rotational corrections or changes ΔX from average spectroscopic parameters of 3-hydroxypropenal along with interaction parameters determined in the present study.

Parameter I	Value I	Value II	Parameter II
		323 523.09353 (185)	$E/\Delta E^{(a)}$
		24.8460491 (130)	$E_K{}^{(b)}$
		−18.7394637 (47)	$E_J{}^{(b)}$
		−4.0806764 (23)	$E_2{}^{(b)}$
A	9839.9556351 (204)	6.1065853 (134)	$\Delta A^{(c)}$
B	5185.6270046 (137)	−26.9008165 (77)	$\Delta B^{(c)}$
C	3393.8067801 (96)	−10.5781109 (51)	$\Delta C^{(c)}$
$D_K \times 10^3$	4.744792 (60)	0.32757 (108)	$(E_{KK}/-\Delta D_K) \times 10^3$
$D_{JK} \times 10^3$	−3.449702 (41)	−0.79152 (112)	$(E_{JK}/-\Delta D_{JK}) \times 10^3$
$D_J \times 10^3$	3.1237538 (65)	0.455189 (37)	$(E_{JJ}/-\Delta D_J) \times 10^3$
$d_1 \times 10^3$	−1.2433617 (32)	0.1810947 (22)	$(E_{2J}/\Delta d_1) \times 10^3$
$d_2 \times 10^3$	−0.1596366 (14)	0.018008 (18)	$(E_4/\Delta d_2) \times 10^3$
$H_K \times 10^9$	46.4796 (265)	−18.450 (105)	$(E_{KKK}/\Delta H_K) \times 10^9$
$H_{KJ} \times 10^9$	−73.3040 (243)	6.817 (140)	$(E_{JKK}/\Delta H_{KJ}) \times 10^9$
$H_{JK} \times 10^9$	39.0206 (109)	15.617 (41)	$(E_{JJK}/\Delta H_{JK}) \times 10^9$
$H_J \times 10^9$	−5.34499 (167)	−4.29228 (125)	$(E_{JJJ}/\Delta H_J) \times 10^9$
$h_1 \times 10^9$	−1.99143 (83)	−2.18286 (75)	$(E_{2JJ}/\Delta h_1) \times 10^9$
$h_2 \times 10^9$	0.354894 (173)	−0.35670 (38)	$(E_{4J}/\Delta h_2) \times 10^9$
$h_3 \times 10^9$	0.097037 (72)	−0.065374 (202)	$(E_6/\Delta h_3) \times 10^9$
$L_K \times 10^{15}$	−300.7 (87)	763.3 (172)	$(E_{KKKK}/\Delta L_K) \times 10^{15}$
$L_{KKJ} \times 10^{15}$	416.7 (109)	−1124.1 (250)	$(E_{JKKK}/\Delta L_{KKJ}) \times 10^{15}$
$L_{JK} \times 10^{15}$	−45.9 (58)	685.3 (134)	$(E_{JJKK}/\Delta L_{JK}) \times 10^{15}$
$L_{JJK} \times 10^{15}$	−108.45 (169)	−325.9 (32)	$(E_{JJJK}/\Delta L_{JJK}) \times 10^{15}$
$L_J \times 10^{15}$	19.254 (158)	−23.883 (163)	$(E_{JJJJ}/\Delta L_J) \times 10^{15}$
$l_1 \times 10^{15}$	9.019 (79)	−21.516 (84)	$(E_{2JJJ}/\Delta l_1) \times 10^{15}$
$l_2 \times 10^{15}$		−11.114 (59)	$(E_{4JJ}/\Delta l_2) \times 10^{15}$
$l_3 \times 10^{15}$	0.3182 (118)		$(E_{6J}/\Delta l_3) \times 10^{15}$
$l_4 \times 10^{15}$	−0.1252 (34)	0.1665 (34)	$(E_8/\Delta l_4) \times 10^{15}$
F_{ab}	45.3158 (32)		
$F_{ab,K} \times 10^6$	−728.03 (70)		
$F_{ab,J} \times 10^6$	906.35 (37)		
$F_{2ab} \times 10^6$	53.629 (249)		
$F_{ab,KK} \times 10^9$	−11.738 (74)		
$F_{ab,JK} \times 10^9$	27.0669 (272)		
$F_{2ab,J} \times 10^9$	7.9407 (224)		
$F_{ab,JKK} \times 10^{12}$	0.1050 (91)		
$F_{ab,JJK} \times 10^{12}$	−0.9419 (40)		

Notes. Watson's S reductions was used in the representation I^r. Numbers in parentheses are one standard deviation in units of the least significant figures. All parameters are defined positively, except D_K, D_{JK}, D_J, and their differences. Empty fields indicate parameters not used in the final fit. Parameters X and interaction parameters F_{ab} etc. are listed under headings Parameter I and Value I; the ΔX, which can be interpreted as rotational corrections to E, are given under the headings Value II and Parameter II. $^{(a)}E(0^-) - E(0^+) = 2E = 2\Delta E = 647046.1871$ (37) MHz or 21.58313759 (12) cm^{-1} per definition of E and ΔE, see sect. 4.1. $^{(b)}$Applied in the fit with rotational corrections to the energies. $^{(c)}$Applied in the fit with differences in spectroscopic parameters.

are 1066 transitions from $v = 0^+$ to $v = 0^-$, mostly with $\Delta K_a = 0$, some with $\Delta K_a = -2$, and even fewer with $\Delta K_a = -4$ or -6. And finally there are 235 transitions from $v = 0^-$ to $v = 0^+$, mostly with $\Delta K_a = +4$ and $+2$, but also 16 having $\Delta K_a = +6$. The line list also contains 79 lines from Baughcum et al. (1981) and 11 lines from Stolze et al. (1983), see also Sect. 4.2.

The final set of spectroscopic parameters is presented in Table 1. The rms of our lines is 17.4 kHz, and the rms error is 0.838. The rms of the previous data from Baughcum et al. (1981) and from Stolze et al. (1983) is 8.9 kHz and 7.4 kHz, respectively. The rms of 17.3 kHz and the rms error of 0.839 for the total fit are obviously dominated by our data.

The line, parameter, and fit file, along with auxiliary files, are available in the fitting spectra section[1] of the CDMS. A calculation of the rotation-tunneling spectrum is deposited in

[1] https://cdms.astro.uni-koeln.de/classic/predictions/pickett/beispiele/3-HP/

the catalog section[2] of the CDMS. The line list with quantum numbers, uncertainties and residuals between observed frequencies and those calculated from the final set of spectroscopic parameters is available from ads.

5. Discussion of the laboratory spectroscopic results

It is somewhat easier to compare the differences in spectroscopic parameters with the respective spectroscopic parameters. The lowest order parameters ΔA, ΔB, and ΔC are comparatively large, though still much smaller than A, B, and C because the tunneling barrier is relatively low, and the splitting between $v = 0^+$ and $v = 0^-$ is relatively large. It is very common that the ratio of the differences in spectroscopic parameters with the respective spectroscpic parameters increases with order of magnitude of the parameters. The differences are only about an order of magnitude smaller in case of the quartics, similar in magnitude for the sextics, and mostly slightly larger in case of the octics. The number of transitions within each tunneling state are much larger than those between the tunneling states. Therefore, it is not surprising that the absolute uncertainties of the changes in the distortion parameters are mostly larger than those of the respective parameters; however, it is opposite in the case of the rotational parameters.

The spectroscopic parameters from the present work are accurate enough for all types of radio observations. A calculation at 300 K up to 1.5 THz contains only very few lines with calculated uncertainties exceeding 0.1 MHz; these very few lines should probably be viewed with some caution. This is very different to the line list prior to this work. A calculated spectrum at 125 K contained several fairly strong transitions with uncertainties of around 10 MHz in the range of the PILS data; these transitions are only about a factor of 5 weaker than the strongest transitions in this range. These are a-type transitions with low values of K_a and $\Delta K_a = 2$; their presently calculated frequencies differ by about three times the initial uncertainties. Several other fairly strong transitions had uncertainties around 1 MHz or more, and deviations of up three times these uncertainties are quite common. Stick spectra of the rotational and rotation-tunneling transitions are shown in Fig. 6. While the rotation-tunneling transitions are usually much weaker, relatively strong transitions appear in the 300 to 700 GHz region.

The rotation of the RAS with respect to the principal inertial axis system is derived as $\sin 2\theta = 2F_{ab}/(A - B)$ (Pickett 1972). Its value of 0.557884 (39)° appears to be a fairly typical one. Data derived for selected other molecules are, for example, 0.8390° (ab-plane) and 1.7892° (bc) for aGg'-ethylene glycol (Christen & Müller 2003), as well as 0.073° (ac) and 0.286° (bc) for propargyl alcohol (Pearson & Drouin 2005).

A comparison of our present spectroscopic parameters with those from previous work is meaningful for low order parameters. The rotation-tunneling interaction was considered by Turner et al. (1984), by Firth et al. (1991), and by Baba et al. (1999). Rotational and quartic centrifugal distortion parameters, the energy difference, the interaction parameter F_{ab}, and its distortion correction $F_{ab,J}$ were determined in all three studies. The agreement among the rotational parameters is good, while the agreement is only good for the quartic parameters from the latest study (Baba et al. 1999) and reasonable in the case of the other two studies. It is instructive to compare the energy differences

[2] https://cdms.astro.uni-koeln.de/classic/entries/

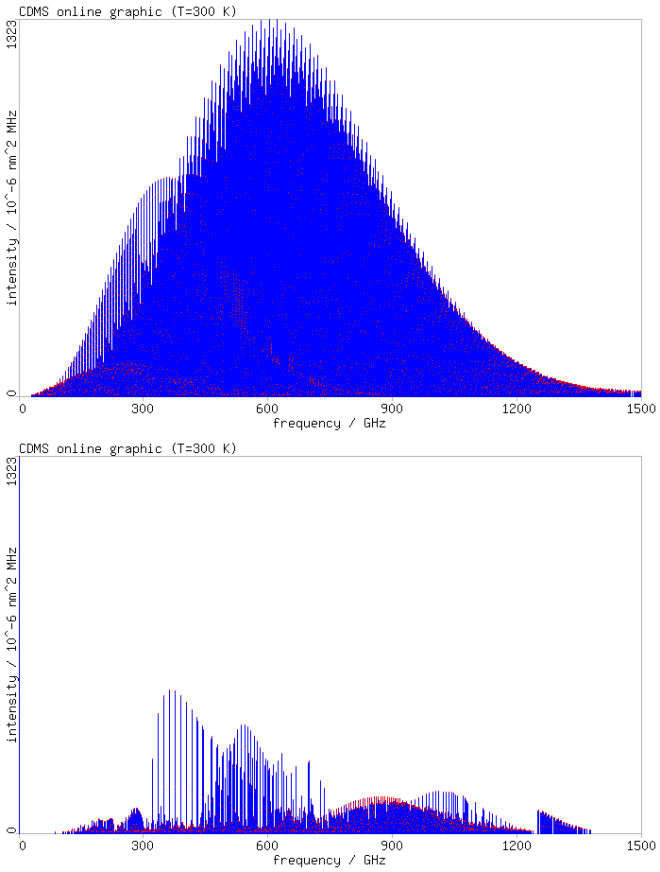

Fig. 6. Stick spectra of 3-hydroxypropenal. The upper trace shows the rotational transitions with b-type selection rules, and the lower trace displays the rotation-tunneling transitions with a-type selection rules.

and interaction parameters from previous work with ours. The energy differences are 647049 (12) MHz (Turner et al. 1984), 647094.9 (51) MHz (Firth et al. 1991), and 647046.208 (19) MHz (Baba et al. 1999), compared to 647046.1871 (37) MHz from our study. The agreement is excellent in the case of the latest study and reasonable for the earlier ones; the smaller uncertainties reflect to some degree the extent of the corresponding data set. The interaction parameters in the same order are 45.51 (4) MHz, 46.01 (2) MHz, and 45.8965 (82) MHz, compared to 45.3158 (32) MHz from our study. The agreement is fairly good in all cases, the somewhat large deviation from the latest study with respect to the combined uncertainties is probably caused by a much larger set of parameters needed to fit our very large data set. Firth et al. (1991) also reported a nearly full set of sextic distortion parameters while Baba et al. (1999) reported a set of four diagonal distortion parameters for each tunneling state plus a value for $F_{ab,K}$; the agreement with our values is reasonable.

Baughcum et al. (1984) evaluated the tunneling barrier height for the main isotopolog as ~6.6 kcal mol^{-1} or ~2300 cm^{-1}. While the authors pointed out that the small amount of data for the main isotopic species leads to a great uncertainty of this barrier height, we note that we are not aware of later attempts to determine the barrier height in similar ways with more data, possibly because the methods were deemed to be too simple. The ~6.6 kcal mol^{-1} may be compared with 4.1 kcal mol^{-1} or about 1400 cm^{-1} derived from a theoretical potential energy surface (PES) (Wang et al. 2008).

The accurate derivation of tunneling splittings from theoretical PESs is challenging. Wang et al. (2008) present ground state splittings of 21.6 and 22.6 cm^{-1} from calculations in Cartesian and normal coordinates, respectively, with estimated uncertaities of 2–3 cm^{-1}. Both values compare very favorably with our present 21.58313759 (12) cm^{-1}, which in turn is very similar to most earlier, less accurate values, as discussed further above. Lüttschwager et al. (2013) determined experimentally tunneling splittings in excited vibrational states of 3-hydroxypropenal and compare the values with those from several theoretical calculations. While the agreement is in all but one instances very good for the ground state splitting, the agreement is less favorable in excited vibrational states.

6. Observations of 3-hydroxypropenal in IRAS16293 B

6.1. Analysis of the ALMA-PILS observations

The 3-hydroxypropenal molecule has been tentatively detected in the solar-type protostar IRAS16293 B by Coutens et al. (2022). The lines have been searched for in PILS carried out with ALMA. This survey covers a large spectral range between 329.1 and 362.9 GHz with an angular resolution of 0.5″ (~60 au) and a spectral resolution of 0.244 MHz (~0.2 km s^{-1}). The data reduction process as well as additional characteristics of the observations are presented in Jørgensen et al. (2016). Thanks to its high sensitivity (rms ≈ 4–5 mJy $beam^{-1}$ per km s^{-1}), a large variety of complex organic molecules have been detected in this survey. Local thermodynamic equilibrium (LTE) models have been carried out to reproduce the observations and derive the column densities and excitation temperatures of the different molecules. In particular, different excitation temperatures have been found in this source. Some molecules, such as NH_2CHO, NH_2CN, CH_3OH, HCOOH, CH_3OCHO, CH_2OHCHO, and CH_3CH_2OH show a high excitation temperature of 300 K (Coutens et al. 2016, 2018; Jørgensen et al. 2018), while others (*c*-C_2H_4O, CH_3CHO, CH_3OCH_3, CH_3CCH, CH_3CN, C_2H_5CN) show a lower excitation temperature of 125 K (Lykke et al. 2017; Jørgensen et al. 2018; Calcutt et al. 2018, 2019). Based on the previous catalog of 3-hydroxypropenal lines, it was not possible to distinguish between an excitation temperature of 125 K and 300 K for this species. Indeed, the lines with high E_{up} that should allow us to constrain the excitation temperature, showed too large frequency uncertainties. Given the very high line density of this survey, it was not possible to know if they were detected. Two column densities were consequently derived: $N = 1.0 \times 10^{15}$ cm^{-2} for $T_{ex} = 125$ K and $N = 1.8 \times 10^{15}$ cm^{-2} for $T_{ex} = 300$ K.

The results of this new spectroscopic study enable us to search for the lines of 3-hydroxypropenal of high excitation. We ran two LTE models with the previously derived best-fit parameters and compared them to the observations. A similar result is obtained for the 11 lines attributed to 3-hydroxypropenal, which showed moderate E_{up} values (<300 K) and small frequency uncertainties (see Fig. 2 of Coutens et al. 2022). If we check the full survey, no major issue is seen for the model with $T_{ex} = 125$ K. However, the model with $T_{ex} = 300$ K and $N = 1.8 \times 10^{15}$ cm^{-2} does not reproduce the observations. Indeed, several undetected lines (~30) are predicted above 3σ with this model (see Fig. 7). A better agreement would be obtained if we lower the column density at 1.0×10^{15} cm^{-2}. But several detected lines (Fig. 2 of Coutens et al. 2022) are in that case under-produced in terms of intensity. In summary, an excitation temperature of 125 K is more appropriate than 300 K for this species.

Even if we do not detect any high excitation lines of 3-hydroxypropenal in the PILS data, it is important to note that such a spectroscopic study is useful, not only to constrain the excitation temperature of the molecule in IRAS16293 B but also for its search in other sources with potentially higher excitation temperatures. The shift of some of the high excitation lines of 3-hydroxypropenal is significant. For example, in Fig. 8, we show that previous high excitation transitions that were matching some line emission in IRAS16293 B are now predicted in areas free of lines. A proper line identification of this molecule in other sources is now possible.

6.2. Search for additional transitions of 3-hydroxypropenal in the ALMA archive

We searched the ALMA archive for projects possibly covering additional transitions to further strengthen the assignment of 3-hydroxypropenal toward IRAS16293 B. We used the ATOMIS[3] web application (Coutens et al. 2023) to list all the ALMA archival observations that cover transitions of 3-hydroxypropenal with $A_{ij} \geq 5 \times 10^{-4}$ s^{-1} and $E_{up} \leq 500$ K. The angular resolution was limited to the range 0.3–0.7″ so that it is relatively close to the PILS resolution (~0.5″). We requested data with a sensitivity better than 10 mJy $beam^{-1}$ for a bin width of 1 km s^{-1} and only selected observational results with a spectral resolution better than 0.5 km s^{-1}. Table 2 summarizes the observational projects that cover such transitions (apart from the PILS project).

After checking the weblog for each project, we downloaded the FITS cubes provided on the ALMA archive for all the listed transitions and extracted the spectra at the position studied in PILS ($\alpha_{J2000} = 16^h32^m22\overset{s}{.}58$, $\delta_{J2000} = -24°28'32.8''$). For the project 2013.1.00061.S, the data that we used are those reduced by Andreu et al. (in prep.) with a restoring beam of 0.5″ similar to what has been done for PILS. We could clearly see that the continuum was not properly subtracted at the extracted position for two spectral windows of the project 2022.1.00554.S (296.4 and 309.7 GHz). We corrected it by fitting a one-order polynomial fit on the channels that do not seem to show any line emission.

In total, thanks to the ALMA archival data, we detected seven additional lines of 3-hydroxypropenal with a signal-to-noise ratio of about 3σ or more (see Fig. 9). The model derived with the PILS data is in very good agreement with the observations. Figure 10 shows the lines that are not detected. These transitions are not detected either because their predicted intensities are too faint compared to the noise level or because they are blended with other species. Table 2 summarizes for each transition if the line is detected or not with, in the latter case, the reason for the non-detection. With this new spectroscopic study, the seven additional detected transitions and the good agreement of their intensities with the model, the detection of HOCHCHCHO can now be considered as secure. The excitation temperature of ~125 K and the column density of $\sim 1.0 \times 10^{15}$ cm^{-2} of this molecule are also reliable, which provides useful constraints for chemical models (Coutens et al. 2022).

7. Conclusions and outlook

We have obtained a very large line list of the tunneling-rotation spectrum of 3-hydroxypropenal in the course of the present investigation that covers large frequency regions and, more

[3] ALMA archive TOol for Molecular Investigations in Space, https://atomis.irap.omp.eu/

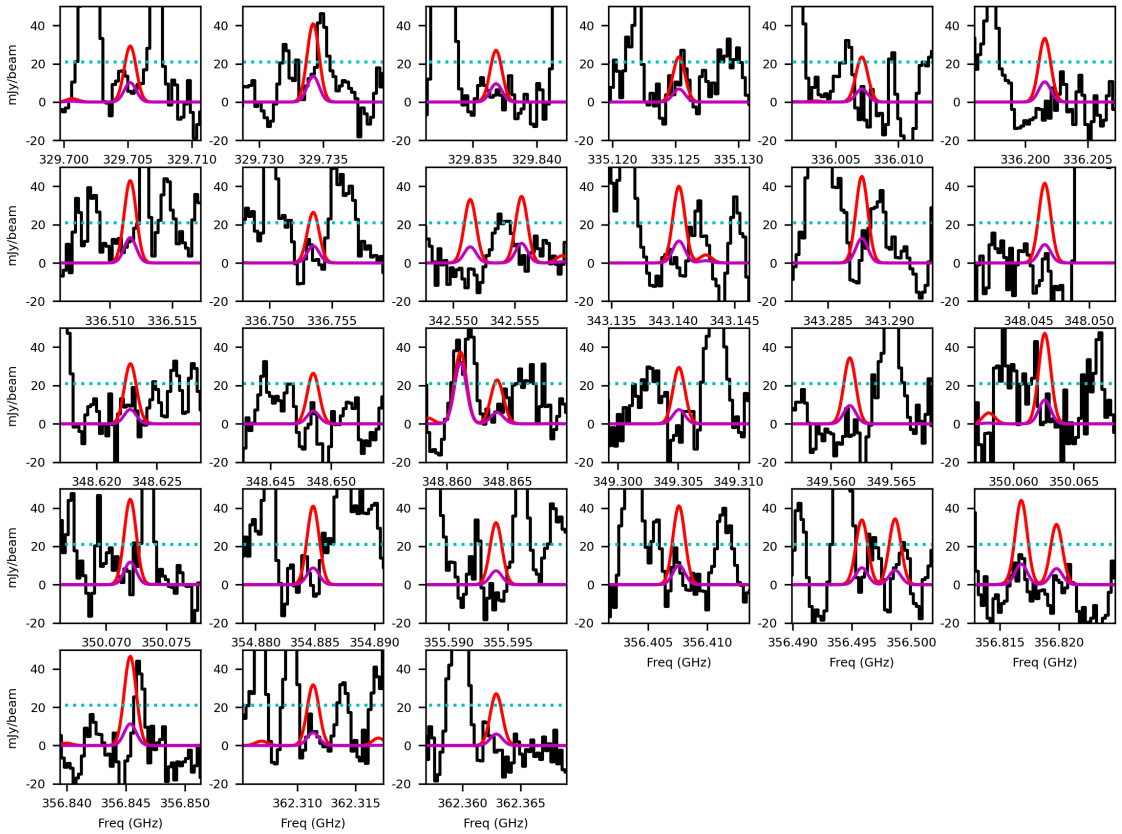

Fig. 7. Undetected lines of 3-hydroxypropenal that are predicted above 3σ with the new spectroscopic data and the parameters previously constrained by Coutens et al. (2022) for an excitation temperature T_{ex} = 300 K. The PILS observations are in black. The model in red has been obtained with the best-fit parameters derived by Coutens et al. (2022) for T_{ex} = 300 K, i.e. with a column density $N = 1.8 \times 10^{15}$ cm^{-2}. For comparison, the model obtained for T_{ex} = 125 K ($N = 1.0 \times 10^{15}$ cm^{-2}) is added in magenta. The cyan dotted line represents the 3 rms level per 0.33 km s^{-1} (1/3 of the line width).

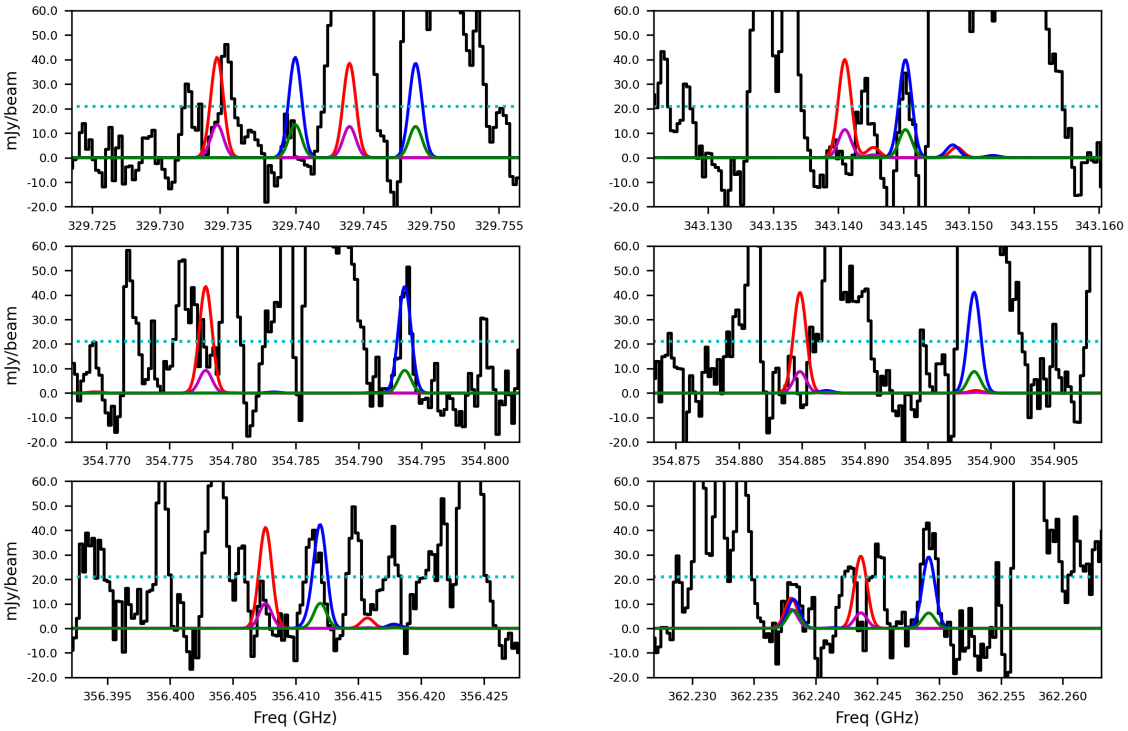

Fig. 8. Examples of high excitation transitions of 3-hydroxypropenal that have been significantly shifted with the new spectroscopic study. Models obtained with previous spectroscopy are indicated in blue (T_{ex} = 300 K) and green (T_{ex} = 125 K). The new models are in red (T_{ex} = 300 K) and magenta (T_{ex} = 125 K). The column densities are $N = 1.0 \times 10^{15}$ cm^{-2} for T_{ex} = 125 K and $N = 1.8 \times 10^{15}$ cm^{-2} for T_{ex} = 300 K. An absorption due to a nearby bright line is present around 343.14 GHz. The cyan dotted line represents the 3 rms level per 0.33 km s^{-1} (1/3 of the line width).

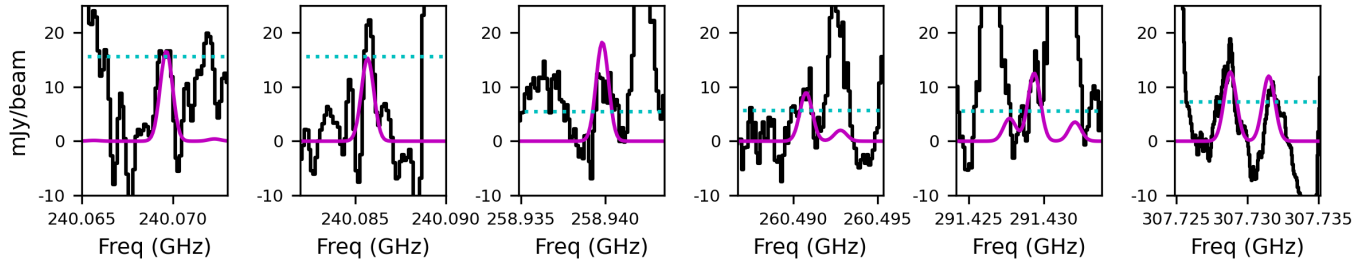

Fig. 9. Detected lines of 3-hydroxypropenal found in the ALMA archive (in black). The model in magenta corresponds to $N = 1.0 \times 10^{15}$ cm^{-2}, $T_{ex} = 125$ K, a source size of 0.5″ and a FWHM of 1 km s^{-1}. The cyan dotted line represents the 3 rms level per 0.33 km s^{-1} (1/3 of the line width).

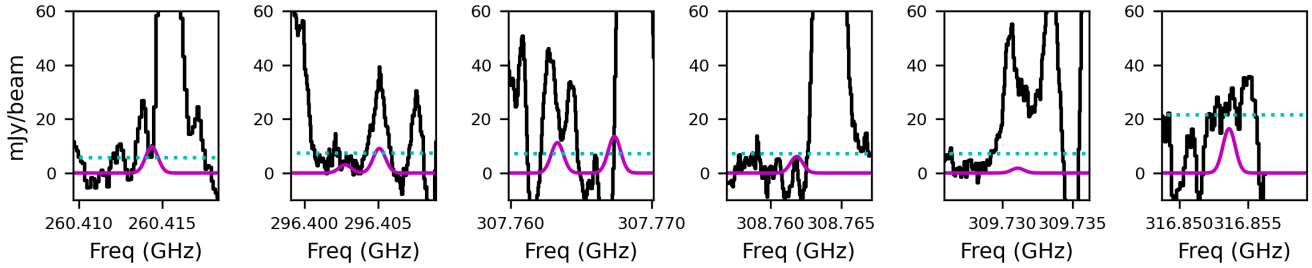

Fig. 10. Non-detected lines of 3-hydroxypropenal in the ALMA archive (in black). The model in magenta corresponds to $N = 1.0 \times 10^{15}$ cm^{-2}, $T_{ex} = 125$ K, a source size of 0.5″ and a FWHM of 1 km s^{-1}. The cyan dotted line represents the 3 rms level per 0.33 km s^{-1} (1/3 of the line width).

Table 2. Observations covering transitions of 3-hydroxypropenal in the ALMA archive.

Transition $J', K'_a, K'_c(v'_t) - J'', K''_a, K''_c(v''_t)$	Frequency (GHz)	E_{up} (K)	A_{ij} ($\times 10^{-4}$ s^{-1})	Project	Ang. res. (″ × ″)	Comments
35,0,35 (0$^-$)–34,1,34 (0$^-$)	240.06964	241.3	5.1	2021.1.01164.S	0.71 × 0.45	Detected
35,1,35 (0$^-$)–34,0,34 (0$^-$)	240.06964	241.3	5.1	2021.1.01164.S	0.71 × 0.45	–
34,1,33 (0$^-$)–33,2,32 (0$^-$) [a]	240.08569	240.5	4.8	2021.1.01164.S	0.71 × 0.45	Detected
34,2,33 (0$^-$)–33,1,32 (0$^-$) [a]	240.08569	240.5	4.8	2021.1.01164.S	0.71 × 0.45	–
14,13,1 (0$^+$)–13,12,2 (0$^+$)	258.93983	88.4	5.7	2017.1.01565.S	0.45 × 0.37	Detected
14,13,2 (0$^+$)–13,12,1 (0$^+$)	258.93983	88.4	5.7	2017.1.01565.S	0.45 × 0.37	–
35,4,32 (0$^-$)–34,3,31 (0$^-$)	260.41436	273.4	5.4	2017.1.01565.S	0.45 × 0.37	Blended with $HCOOCH_3$
35,3,32 (0$^-$)–34,4,31 (0$^-$)	260.41436	273.4	5.4	2017.1.01565.S	0.45 × 0.37	and CHD(OH)CHO
34,5,30 (0$^-$)–33,4,29 (0$^-$)	260.49075	270.5	5.0	2017.1.01565.S	0.45 × 0.37	Detected
34,4,30 (0$^-$)–33,5,29 (0$^-$)	260.49075	270.5	5.0	2017.1.01565.S	0.45 × 0.37	–
19,12.8 (0$^+$)–18,11,7 (0$^+$) [b]	291.42772	117.9	5.2	2017.1.01565.S	0.41 × 0.37	Noise
19,12.7 (0$^+$)–18,11,8 (0$^+$) [b]	291.42936	117.9	5.2	2017.1.01565.S	0.41 × 0.37	Detected
36,7,29 (0$^+$)–35,8,28 (0$^+$) [b]	296.40275	295.1	5.9	2022.1.00554.S	0.59 × 0.47	Noise
36,8,29 (0$^+$)–35,7,28 (0$^+$) [b]	296.40508	295.1	5.9	2022.1.00554.S	0.59 × 0.47	Blended with U-line
43,2,41 (0$^-$)–42,3,40 (0$^-$)	307.72880	372.2	9.9	2022.1.00554.S	0.57 × 0.46	Detected
43,3,41 (0$^-$)–42,2,40 (0$^-$)	307.72880	372.2	9.9	2022.1.00554.S	0.57 × 0.46	–
42,3,39 (0$^-$)–41,4,38 (0$^-$)	307.73151	370.0	9.4	2022.1.00554.S	0.57 × 0.46	Detected
42,4,39 (0$^-$)–41,3,38 (0$^-$)	307.73151	370.0	9.4	2022.1.00554.S	0.57 × 0.46	with nearby absorption line
41,4,37 (0$^-$)–40,5,36 (0$^-$)	307.76332	370.1	8.8	2022.1.00554.S	0.57 × 0.46	Blended with $^{13}CH_3C(O)CH_3$
41,5,37 (0$^-$)–40,4,36 (0$^-$)	307.76332	370.1	8.8	2022.1.00554.S	0.57 × 0.46	or $SO^{18}O$
44,1,43 (0$^-$)–43,2,42 (0$^-$)	307.76735	373.6	10.4	2022.1.00554.S	0.57 × 0.46	Blended with CH_3CHO
44,2,43 (0$^-$)–43,1,42 (0$^-$)	307.76735	373.6	10.4	2022.1.00554.S	0.57 × 0.46	+ absorption
37,9,29 (0$^-$)–36,8,28 (0$^-$)	308.76184	347.5	6.0	2022.1.00554.S	0.57 × 0.46	Noise
36,10,27 (0$^-$)–35,9,26 (0$^-$)	309.73109	340.4	5.2	2022.1.00554.S	0.56 × 0.45	Blended with CH_3COOH
22,12,11 (0$^+$)–21,11,10 (0$^+$)	316.85362	144.9	5.5	2013.1.00061.S	0.50 × 0.50	Noise

Notes. The following criteria were applied: $A_{ij} \geq 5 \times 10^{-4}$ s^{-1}, $E_{up} \leq 500$ K, a spectral resolution $dv \leq 0.5$ km s^{-1}, an angular resolution between 0.3 and 0.7″, and a sensitivity better than 10 mJy beam^{-1} for a bin width of 1 km s^{-1}. The angular resolutions are taken from the header of the fits datacubes provided on the archive. [a]The transitions at 240.08569 GHz were not listed in the results of ATOMIS but we included them as they are in the same spectral window as the line at 240.06964 GHz and have an E_{up} value close to the limit of 5×10^{-4} s^{-1}. [b]For each pair of close lines, the g_{up} parameters differ significantly despite similar E_{up} and A_{ij}.

importantly, large ranges of quantum numbers. This line list was the basis of an extensive and very accurate set of spectroscopic parameters from which the entire tunneling-rotation spectrum of the molecule in the ground vibrational state can be derived with great accuracy. This new calculation enabled us to settle the issue of the excitation temperature of 3-hydroxypropenal in the warm part of the molecular cloud surrounding the protostar IRAS16293 B, as we were able to rule out $T_{ex} \approx 300$ K and establish $T_{ex} \approx 125$ K. The detection of seven additional lines in the ALMA archive raised the detection from somewhat tentative to secure. With the new data set, it is now possible to search for 3-hydroxypropenal in star-forming regions with considerably higher T_{ex}.

Acknowledgements. This paper makes use of the following ALMA data: ADS/JAO.ALMA#2013.1.00278.S, ADS/JAO.ALMA#2013.1.00061.S, ADS/JAO.ALMA#2017.1.01565.S, ADS/JAO.ALMA#2021.1.00544.S, and ADS/JAO.ALMA#2022.1.00554.S. ALMA is a partnership of ESO (representing its member states), NSF (USA) and NINS (Japan), together with NRC (Canada) and NSC and ASIAA (Taiwan), in cooperation with the Republic of Chile. The Joint ALMA Observatory is operated by ESO, AUI/NRAO and NAOJ. The work in Lille and Rennes was supported by the Programme National "Physique et Chimie du Milieu Interstellaire" (PCMI) of CNRS Terre @ Univers with CNRS Physique & CNRS Chimie, co-funded by CEA and CNES. HSPM acknowledges support by the Deutsche Forschungsgemeinschaft via the collaborative research centers SFB 956 (project ID 184018867), subproject B3, and SFB 1601 (project ID 500700252), subprojects Inf and A4. AC received funding from the European Research Council (ERC) under the European Union's Horizon 2020 research and innovation programme (ERC Starting Grant "Chemtrip", grant agreement no. 949278). JKJ is supported by the Independent Research Fund Denmark (grant number 0135-00123B). Our research benefited from NASA's Astrophysics Data System (ADS).

References

Baba, T., Tanaka, T., Morino, I., Yamada, K. M. T., & Tanaka, K. 1999, J. Chem. Phys., 110, 4131
Baughcum, S. L., Duerst, R. W., Rowe, W. F., Smith, Z., & Wilson, E. B. 1981, J. Am. Chem. Soc., 103, 6296
Baughcum, S. L., Smith, Z., Wilson, E. B., & Duerst, R. W. 1984, J. Am. Chem. Soc., 106, 2260
Calcutt, H., Jørgensen, J. K., Müller, H. S. P., et al. 2018, A&A, 616, A90
Calcutt, H., Willis, E. R., Jørgensen, J. K., et al. 2019, A&A, 631, A137
Christen, D., & Müller, H. S. P. 2003, Phys. Chem. Chem. Phys., 5, 3600
Coutens, A., Jørgensen, J. K., van der Wiel, M. H. D., et al. 2016, A&A, 590, A6
Coutens, A., Willis, E. R., Garrod, R. T., et al. 2018, A&A, 612, A107
Coutens, A., Loison, J. C., Boulanger, A., et al. 2022, A&A, 660, A6
Coutens, A., Ben Hmida, S., & Glorian, J. M. 2023, in SF2A-2023: Proceedings of the Annual meeting of the French Society of Astronomy and Astrophysics, 311
Endres, C. P., Schlemmer, S., Schilke, P., Stutzki, J., & Müller, H. S. P. 2016, J. Mol. Spectrosc., 327, 95
Firth, D. W., Beyer, K., Dvorak, M. A., et al. 1991, J. Chem. Phys., 94, 1812
Isaacson, A. D., & Morokuma, K. 1975, J. Am. Chem. Soc., 97, 4453
Jørgensen, J. K., van der Wiel, M. H. D., Coutens, A., et al. 2016, A&A, 595, A117
Jørgensen, J. K., Müller, H. S. P., Calcutt, H., et al. 2018, A&A, 620, A170
Karlström, G., Wennerström, H., Jónsson, B., et al. 1975, J. Am. Chem. Soc., 97, 4188
Lüttschwager, N. O. B., Wassermann, T. N., Coussan, S., & Suhm, M. A. 2013, Mol. Phys., 111, 2211
Lykke, J. M., Coutens, A., Jørgensen, J. K., et al. 2017, A&A, 597, A53
Margulès, L., McGuire, B. A., Senent, M. L., et al. 2017, A&A, 601, A50
Margulès, L., Motiyenko, R. A., & Demaison, J. 2020, J. Quant. Spec. Radiat. Transf., 253, 107153
Margulès, L., Coutens, A., Ligterink, N. F. W., et al. 2023, MNRAS, 524, 1211
Müller, H. S. P., Schlöder, F., Stutzki, J., & Winnewisser, G. 2005, J. Mol. Struct., 742, 215
Müller, H. S. P., Belloche, A., Xu, L.-H., et al. 2016, A&A, 587, A92
Müller, H. S. P., Garrod, R. T., Belloche, A., et al. 2023, MNRAS, 523, 2887
Pearson, J. C., & Drouin, B. J. 2005, J. Mol. Spectrosc., 234, 149
Pickett, H. M. 1972, J. Chem. Phys., 56, 1715
Pickett, H. M. 1991, J. Mol. Spectrosc., 148, 371
Rowe, W. F. J., Duerst, R. W., & Wilson, E. B. 1976, J. Am. Chem. Soc., 98, 4021
Stolze, M., Hübner, D., & Sutter, D. H. 1983, J. Mol. Struct., 97, 243
Trivella, A., Coussan, S., & Chiavassa, T. 2008, Synth. Commun., 38, 3285
Turner, P., Baughcum, S. L., Coy, S. L., & Smith, Z. 1984, J. Am. Chem. Soc., 106, 2265
Wang, Y., Braams, B. J., Bowman, J. M., Carter, S., & Tew, D. P. 2008, J. Chem. Phys., 128, 224314
Zakharenko, O., Motiyenko, R. A., Margulès, L., & Huet, T. R. 2015, J. Mol. Spectrosc., 317, 41